Nov 10-14, 2025, Salerno, Italy

Multi-strangeness matter from *ab initio* calculations

Hui Tong

Collaborators : Serdar Elhatisari, Ulf-G. Meißner, Zhengxue Ren

Contents

- Introduction
- Hypernuclei and Hypernuclear matter
- Summary and Outlook

Neutron stars

- Neutron stars are one of the densest massive objects in the universe.

J. Schaffner-Bielich, Cambridge University Press (2020)

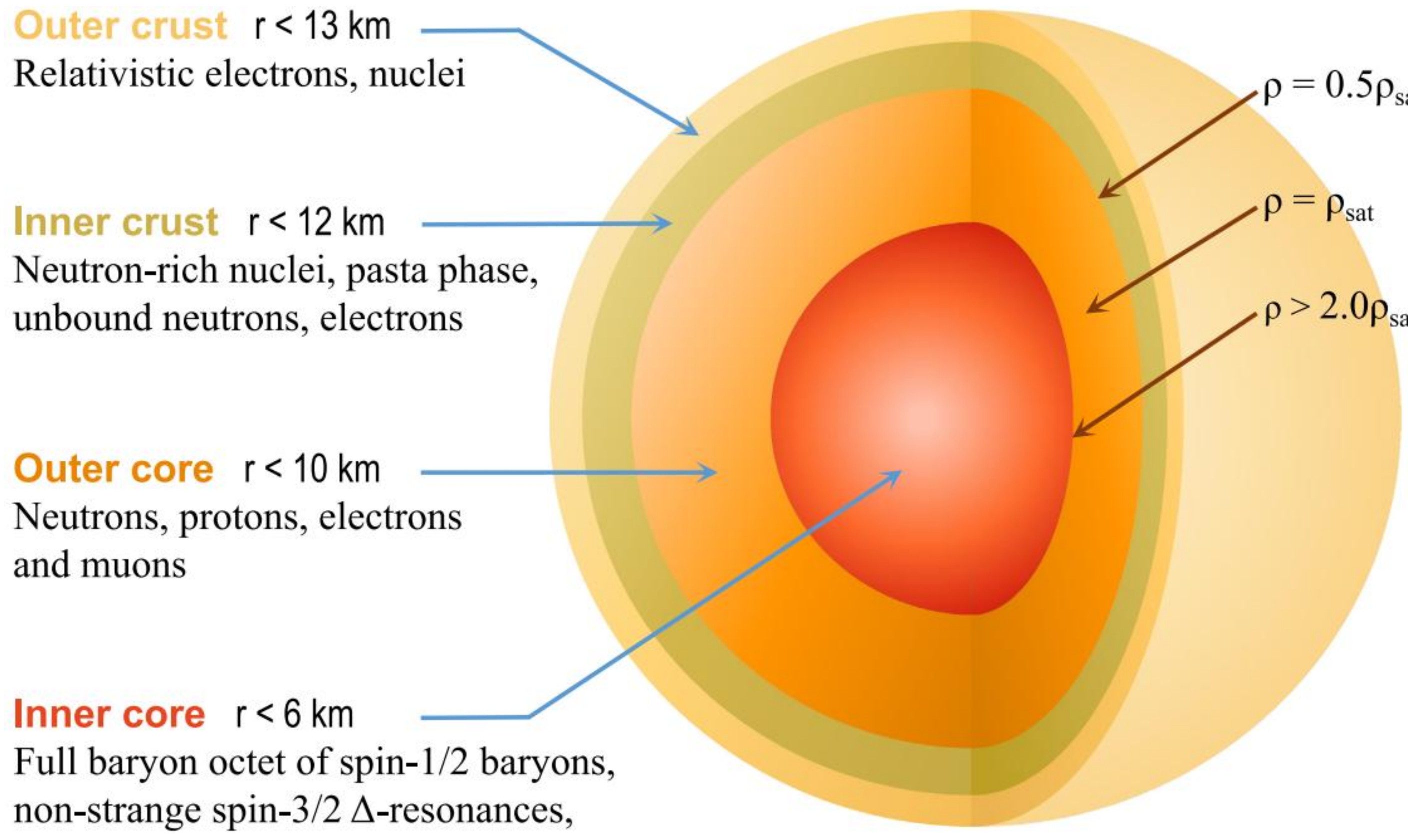

A. Sedrakian, et al., PPNP 131, 104041 (2023)

① Usually refer to a star with a mass on the order of 1-2 solar masses, a radius of 10-12 km.

② The central density can reach several times the empirical nuclear matter saturation density ($\rho_{\rm sat}$≈0.16 $\rm fm^{-3}$).

Neutron star observations and Hyperon puzzle

- Neutron star *mass* measurements.

Figure from Vivek V. Krishnan

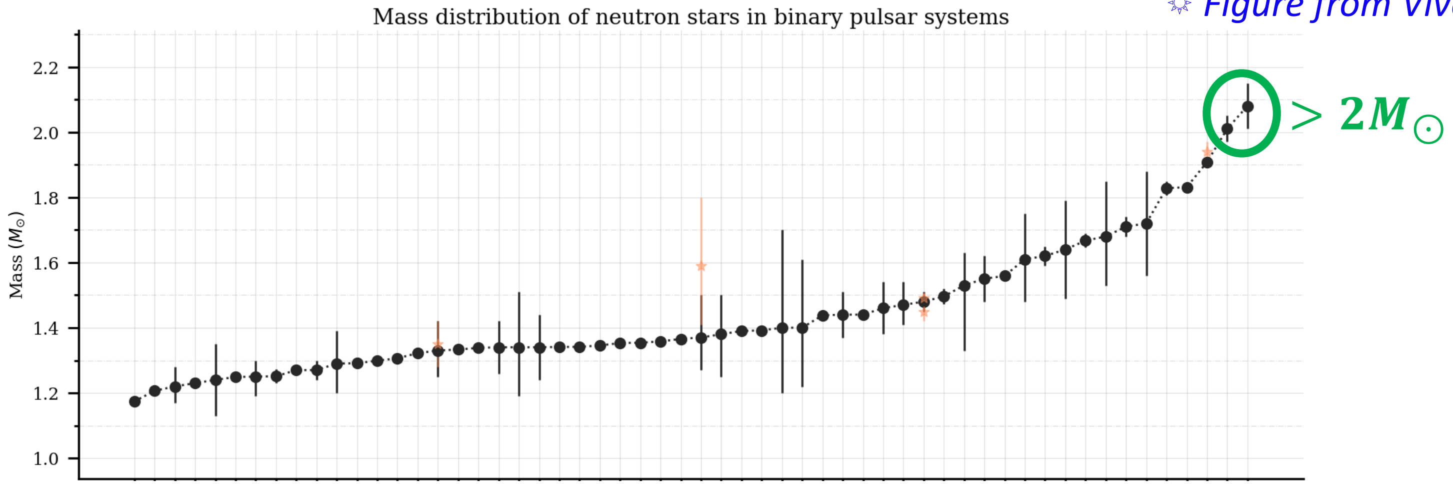

- Some theoretical approaches, such as Brueckner-Hartree-Fock (BHF), predict the appearance of hyperons at $(2-3)\rho_0$, and a softening of the EoS, implying a reduction of the maximum mass.

A. Gal, et al., RMP 88, 035004 (2016)

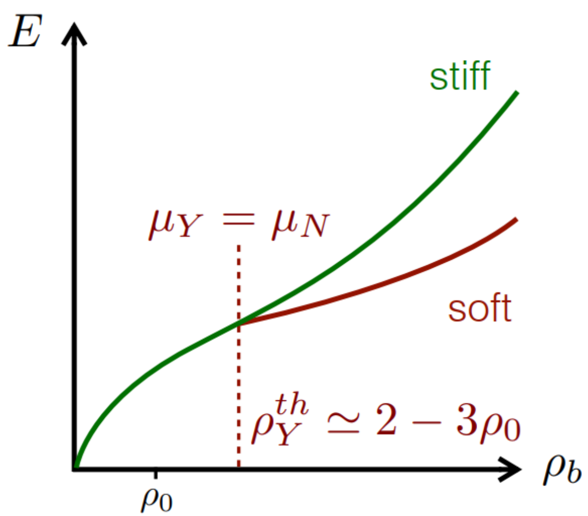

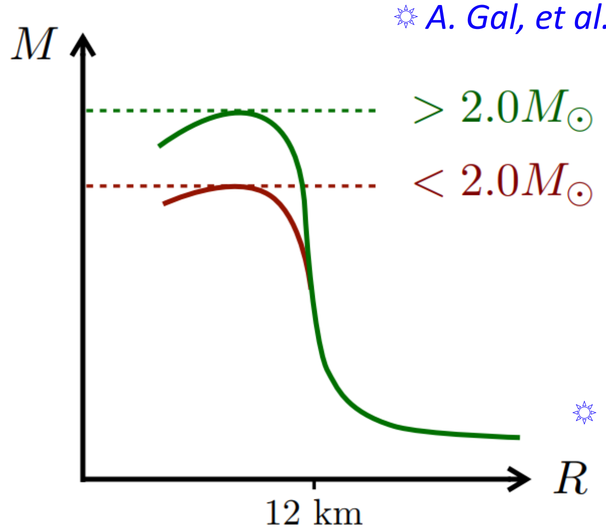

Figure from D. Lonardoni

Hypernuclei and EoS from AFDMC

- Hypernuclei and hyperneutron matter from Auxiliary field diffusion Monte Carlo (AFDMC) with simplified phenomenological interactions.

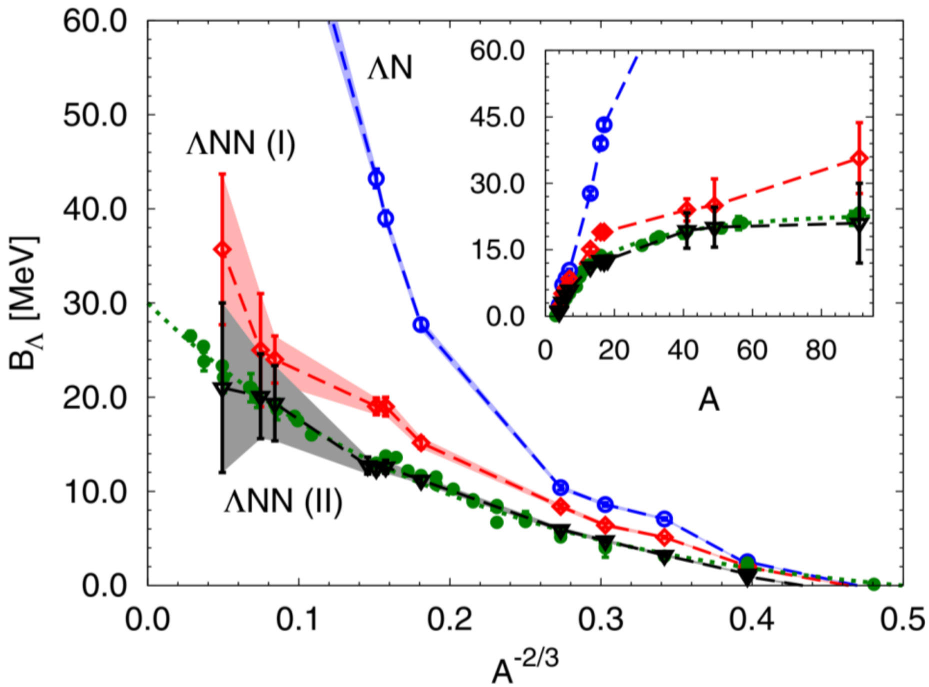

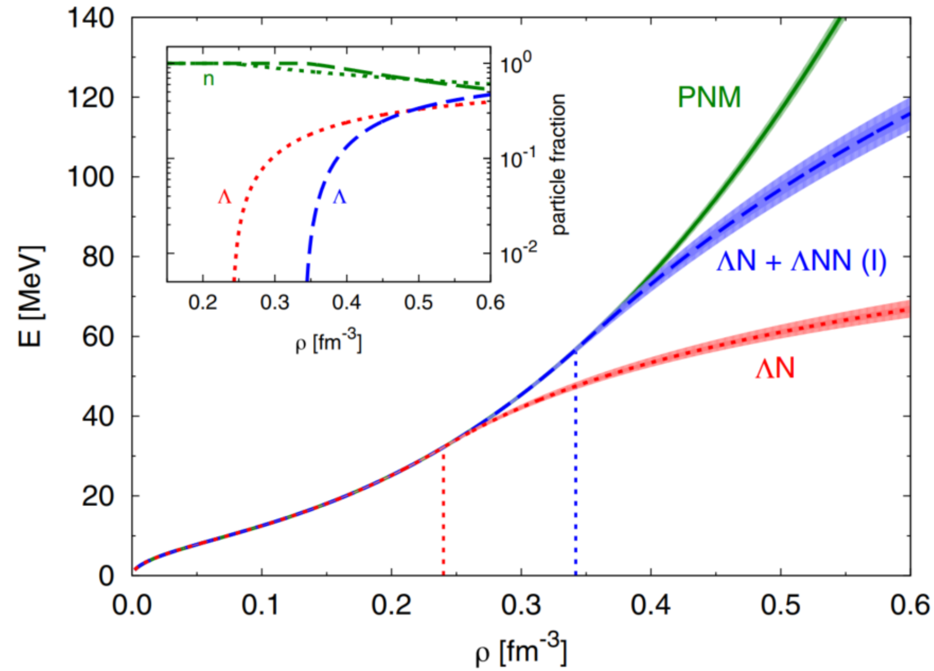

☼ *D. Lonardoni, et al., PRC 89, 014314 (2014)*

☼ *D. Lonardoni, et al., PRL 114, 092301 (2015)*

① $\Lambda NN(I)$: reproduce B_Λ of ${}^{5}_{\Lambda}\mathrm{He}$ and ${}^{17}_{\Lambda}\mathrm{O}$; $\Lambda NN(II)$: reproduce B_Λ up to A=91.

② No protons in hyperneutron matter.

③ Only some fixed number of neutrons (N_n=66, 54, 38) and hyperons (N_Λ=1, 2, 14) are used, the EoS needs to be parametrized.

④ No $\Lambda\Lambda + \Lambda\Lambda N$ interactions.

Neutron star properties from AFDMC

- $\Lambda NN(II)$ can support $2M_{\odot}$, but no Λ present in $2M_{\odot}$ Neutron Star?

D. Lonardoni, et al., PRL 114, 092301 (2015)

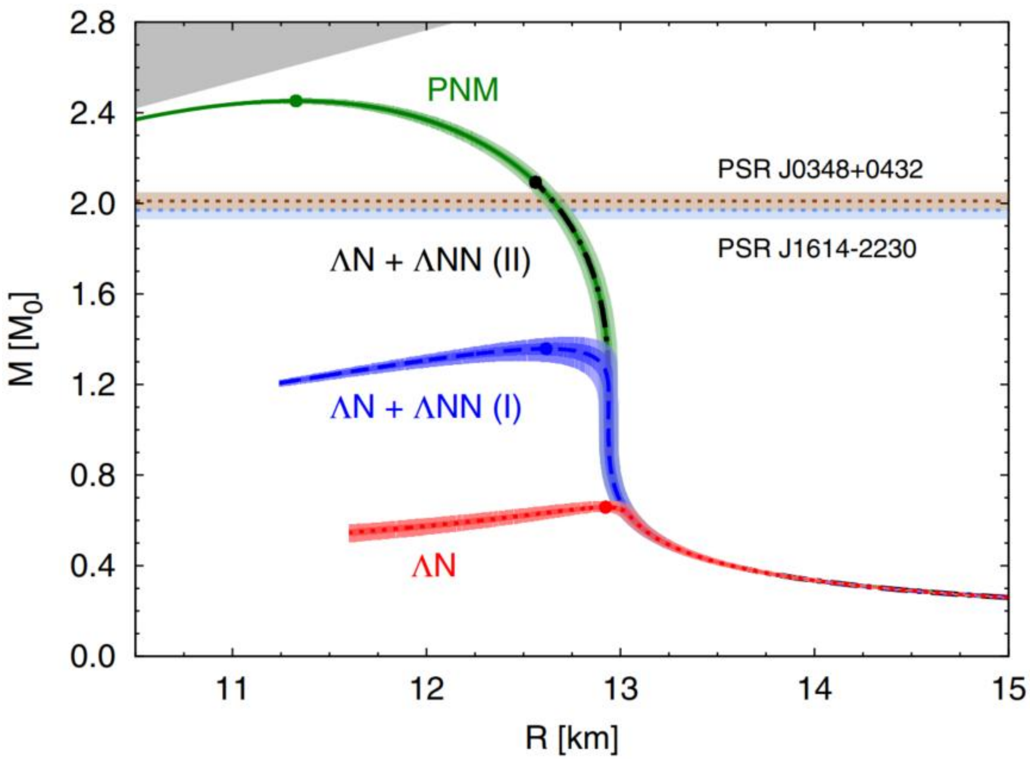

The author concluded that,

① The presence of hyperons in the neutron star core cannot be established.

② The ΛNN force needs additional theoretical investigation, such as chiral perturbation theory.

Hypernuclei and neutron star from BHF

- Hypernuclear matter are calculated from BHF, but only three hypernuclei are calculated from a perturbative many-body approach.

	${}^{41}_{\Lambda}$Ca	${}^{91}_{\Lambda}$Zr	${}^{209}_{\Lambda}$Pb
NSC97a	23.0	31.3	38.8
NSC97a+NNΛ_1	14.9	21.1	26.8
NSC97a+NNΛ_2	13.3	19.3	24.7
NSC97e	24.2	32.3	39.5
NSC97e+NNΛ_1	16.1	22.3	27.9
NSC97e+NNΛ_2	14.7	20.7	26.1
Exp.	18.7(1.1)[†]	23.6(5)	26.9(8)

☼ *D. Logoteta , et al., EPJA 55, 207 (2019)*

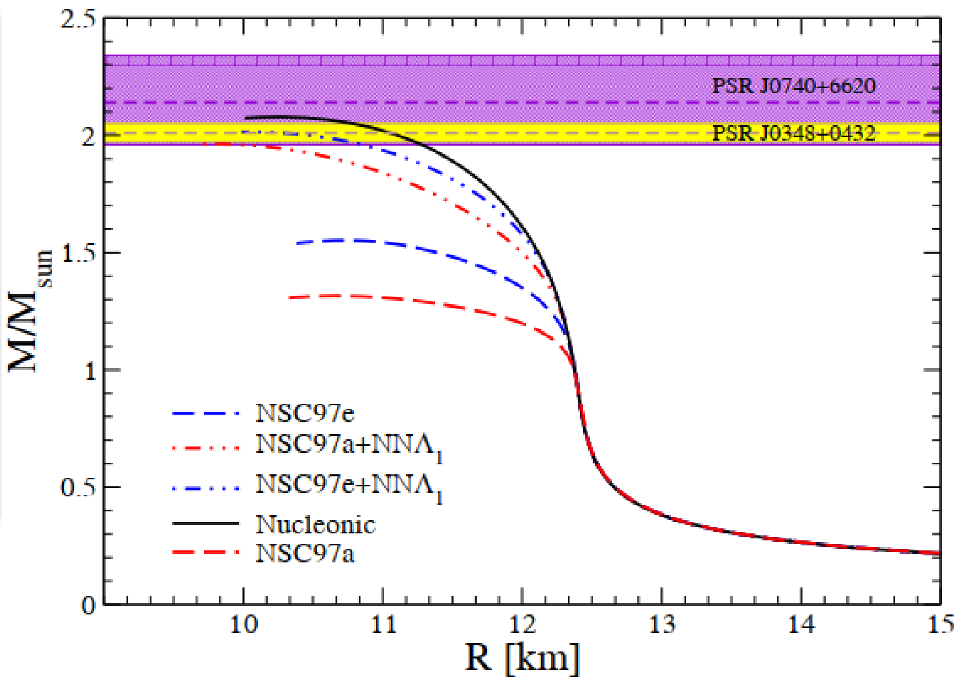

① Not the same framework for hypernuclei and hypernuclear matter.

② The NN, NNN, and NNΛ interactions are adopted from χEFT, but the NΛ interaction from the meson-exchange model.

③ No ΛΛ+ΛΛN interactions.

④ BHF is based on two-hole-line expansions which introduce uncertainties in many-body calculations.

In this work

Any *ab initio* approach that can simultaneously describe hypernuclei across the nuclear chart and hypernuclear matter in neutron stars?

In this work

Any *ab initio* approach that can simultaneously describe hypernuclei across the nuclear chart and hypernuclear matter in neutron stars?

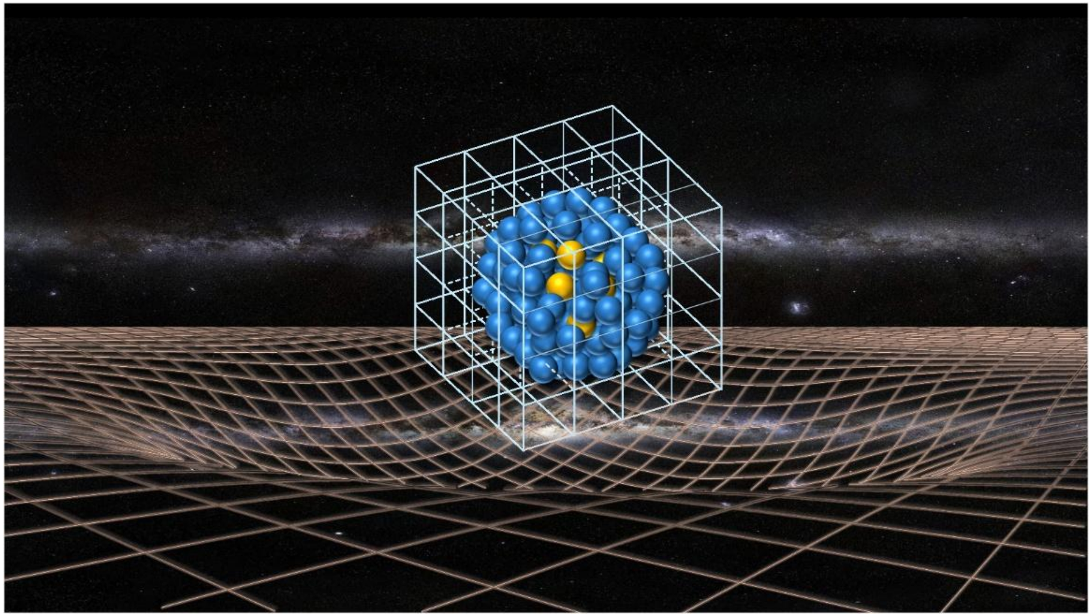

☼ *Figure from Serdar Elhatisari*

1. By combining nuclear lattice EFT with a novel auxiliary-field QMC algorithm, we achieve the first sign-problem free *ab initio* QMC simulations of hypernuclear systems containing arbitrary number of neutrons, protons, and Λs.
2. We present the first *ab initio* calculations that simultaneously describe single- and double-Λ hypernuclei from the light to medium-mass range, the β-stable hypernuclear matter, and neutron star properties.

Contents

The Hamiltonian for nucleons

- Hamiltonian

$$H = H_{\text{free}} + \frac{c_{NN}}{2} \sum_{\vec{n}} : [\tilde{\rho}(\vec{n})]^2 : + \frac{c_{NN}^T}{2} \sum_{I,\vec{n}} : [\tilde{\rho}_I(\vec{n})]^2 : + V_{NN}^{\text{GIR}} + V_{\text{Coulomb}} + V_{NNN}$$

the density operator $\tilde{\rho}(\vec{n})$ is defined as

$$\tilde{\rho}(\vec{n}) = \sum_{i,j=0,1} \tilde{a}_{i,j}^{\dagger}(\vec{n})\, \tilde{a}_{i,j}(\vec{n}) + s_{\text{L}} \sum_{|\vec{n}-\vec{n}'|^2=1} \sum_{i,j=0,1} \tilde{a}_{i,j}^{\dagger}(\vec{n}')\, \tilde{a}_{i,j}(\vec{n}')$$

where i is the spin index, j is the isospin index. The smeared annihilation and creation operators are defined as

$$\tilde{a}_{i,j}(\vec{n}) = a_{i,j}(\vec{n}) + s_{\text{NL}} \sum_{|\vec{n}'-\vec{n}|=1} a_{i,j}(\vec{n}')$$

the s_{L} is a local smearing parameter, s_{NL} is a nonlocal smearing parameter. C_{NN} and C_{NN}^T gives the strength of the two-body interaction. V_{NNN} is the three-body interaction.

Phase shift for nucleons

- The C_{NN} couplings are determined by fitting the phase shift.

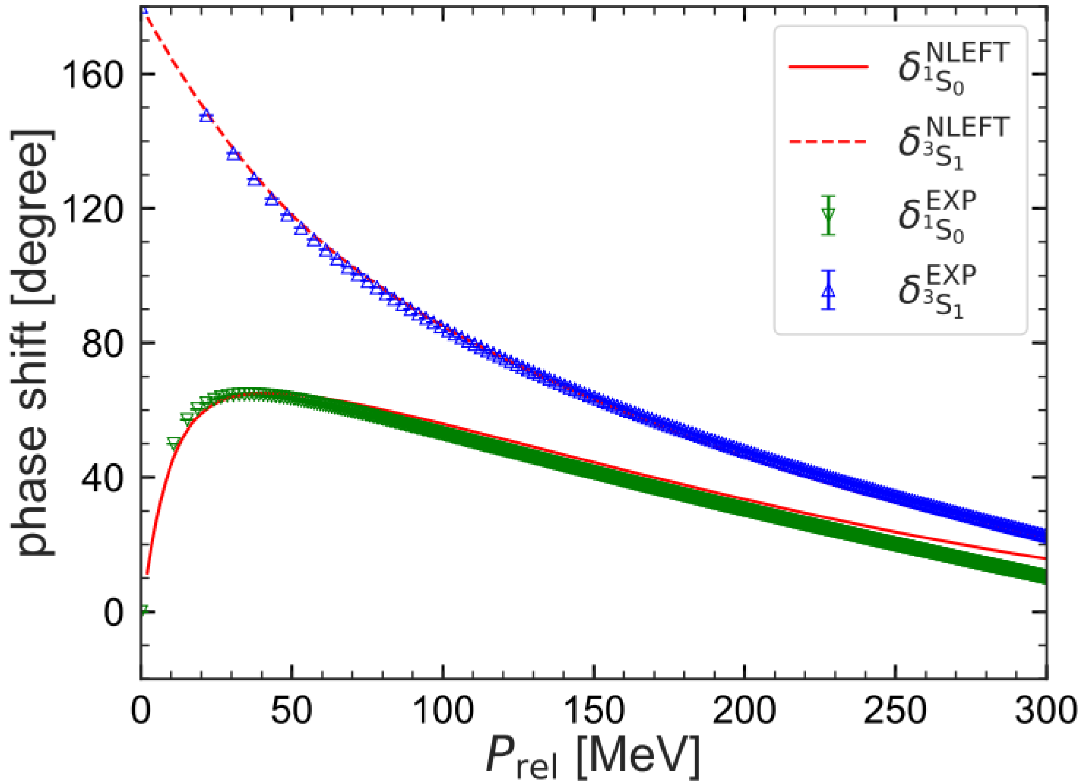

- The Galilean invariance restoration for each channel are obtained by tuning $C_{\mathrm{GIR},i}(i = 0,1,2)$ with the constraint

$$\boxed{C_{\mathrm{GIR},0} + 6C_{\mathrm{GIR},1} + 12C_{\mathrm{GIR},2} = 0}$$

Symmetric Nuclear Matter

- The couplings for three-body interaction are determined by the empirical value for symmetric nuclear matter.

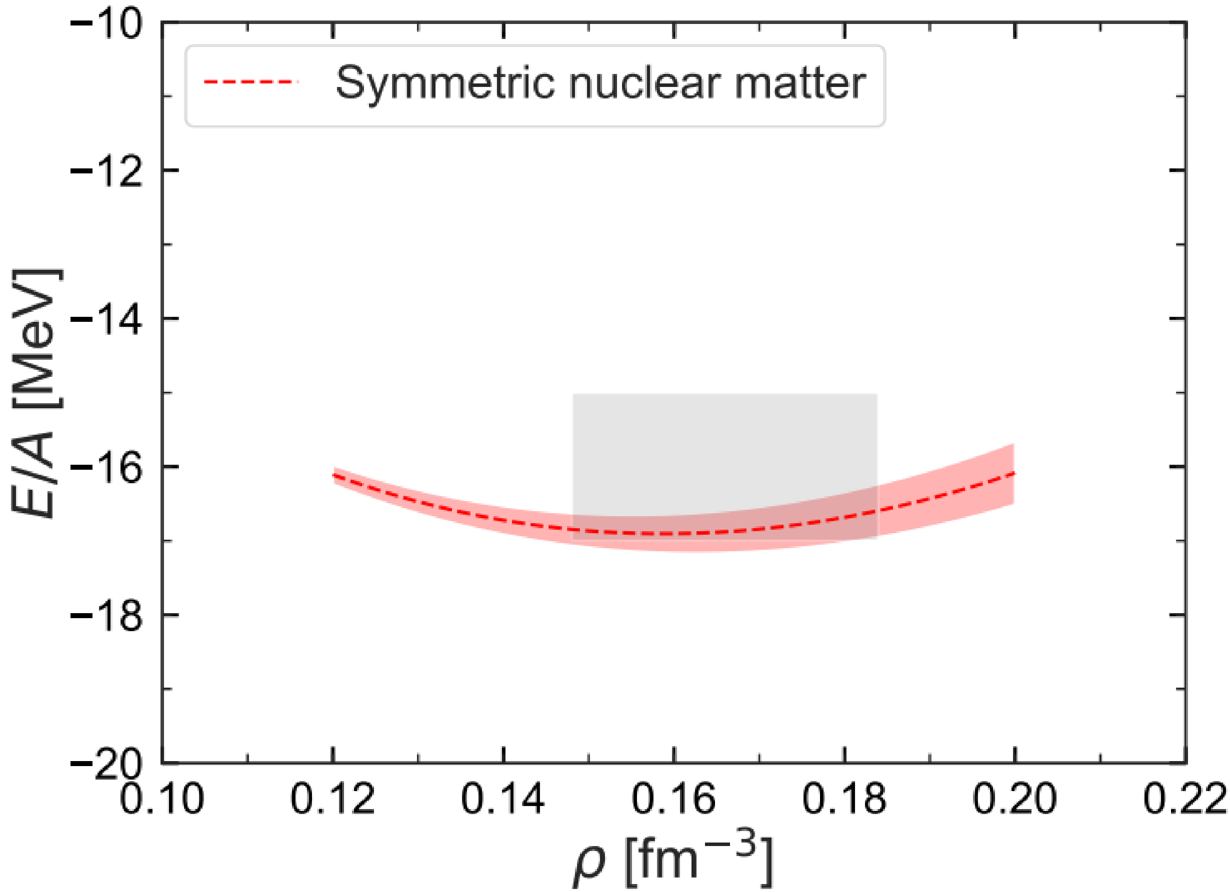

As a prediction, the compression modulus K_∞=229.0(3.6) MeV.

Pure Neutron Matter

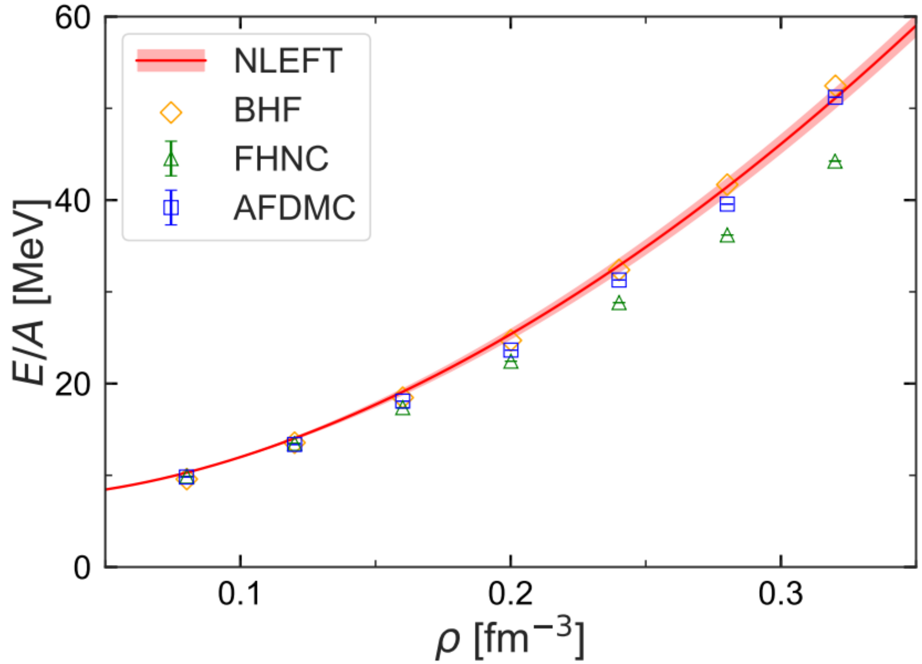

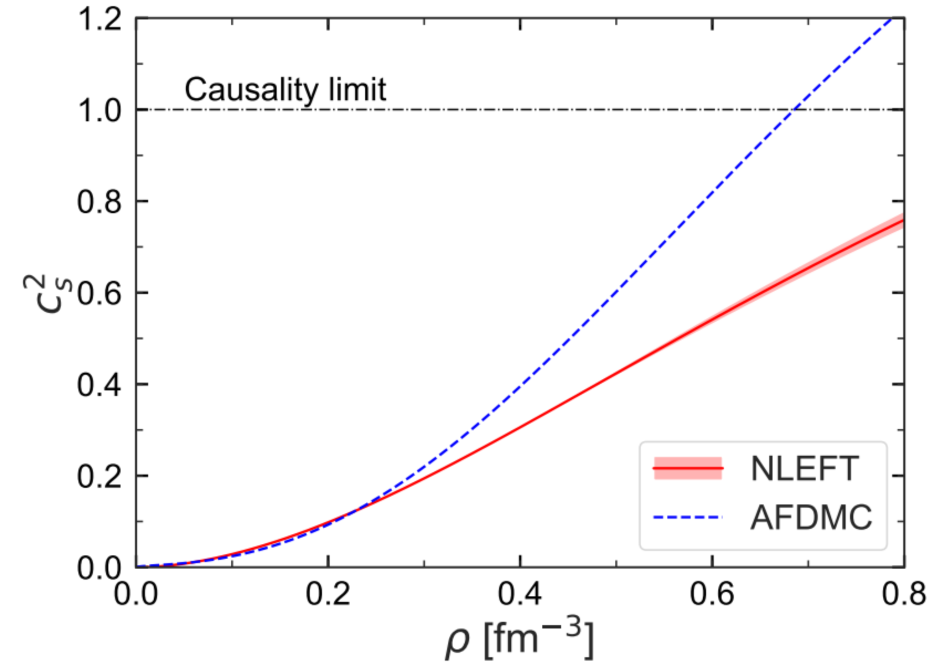

① NLEFT: The calculations are performed by considering up to 232 neutrons in a box to achieve several times the saturation density.

② AFDMC : AV8'+3N interaction inspired by the Urbana IX and the Illinois models, their EoS is stiffer compared to our results and exceeds the causality limit for the speed of sound above $\rho \simeq 0.68\ \mathrm{fm}^{-3}$.

③ The accurate symmetry energy at the saturation density is 33.8 ± 0.6 MeV, and ***no symmetry energy approximation is used*** in our work.

The Hamiltonian for nucleons and hyperons

- For the hyperon-nucleon and hyperon-hyperon interactions, we use minimal interactions. The Hamiltonian is defined as,

$$
\begin{aligned}
H = & H_{\mathrm{free}} + \frac{c_{NN}}{2} \sum_{\vec{n}} : \left[\tilde{\rho}(\vec{n})\right]^2 : + \frac{c_{NN}^T}{2} \sum_{I,\vec{n}} : \left[\tilde{\rho}_I(\vec{n})\right]^2 : \\
& + c_{N\Lambda} \sum_{\vec{n}} : \tilde{\rho}(\vec{n}) \tilde{\xi}(\vec{n}) : + \frac{c_{\Lambda\Lambda}}{2} \sum_{\vec{n}} : \left[\tilde{\xi}(\vec{n})\right]^2 : \\
& + V_{NN}^{\mathrm{GIR}} + V_{N\Lambda}^{\mathrm{GIR}} + V_{\Lambda\Lambda}^{\mathrm{GIR}} + V_{\mathrm{Coulomb}} \\
& + V_{NNN} + V_{NN\Lambda} + V_{N\Lambda\Lambda} ,
\end{aligned}
$$

$C_{N\Lambda}, C_{\Lambda\Lambda}$ give the strength of the two-body interactions. $V_{NN\Lambda}$ and $V_{N\Lambda\Lambda}$ are the three-body interactions. ***We want to*** do the simulation with neutrons, protons and Λs by using ***a single auxiliary field!***

Auxiliary Field for Hypernuclear Systems

- A discrete auxiliary field formulation for the SU(4) interaction,

$$:\exp\left(-\frac{a_t\, c_{NN}}{2}\,\tilde{\rho}^2\right) := \sum_{k=1}^{3} w_k \;:\exp\left(\sqrt{-a_t\, c_{NN}}\, s_k\, \tilde{\rho}\right):$$

  where a_t is the temporal lattice spacing.

- The two-baryon interactions,

$$V_{2\mathrm{B}} = \frac{c_{NN}}{2}\sum_{\vec{n}} :\left[\tilde{\rho}(\vec{n})\right]^2: + c_{N\Lambda}\sum_{\vec{n}} :\tilde{\rho}(\vec{n})\tilde{\xi}(\vec{n}): + \frac{c_{\Lambda\Lambda}}{2}\sum_{\vec{n}} :\left[\tilde{\xi}(\vec{n})\right]^2:$$

  this potential can be rewritten in the following form,

$$V_{2\mathrm{B}} = \frac{c_{NN}}{2}\sum_{\vec{n}} :\left[\tilde{\phi}(\vec{n})\right]^2: + \frac{1}{2}\left(c_{\Lambda\Lambda} - \frac{c_{N\Lambda}^2}{c_{NN}}\right)\sum_{\vec{n}} :\left[\tilde{\xi}(\vec{n})\right]^2:$$

  where $\tilde{\phi} = \tilde{\rho} + \frac{c_{N\Lambda}}{c_{NN}}\tilde{\xi}$, the simulation of system consisting of arbitrary number of nucleons and Λs with a single auxiliary field,

$$:\exp\left(-\frac{a_t\, c_{NN}}{2}\,\tilde{\phi}^2\right) := \sum_{k=1}^{3} w_k \;:\exp\left(\sqrt{-a_t\, c_{NN}}\, s_k\, \tilde{\phi}\right):$$

Couplings for hyperonic interactions

- $C_{N\Lambda}$ is determined by fitting the cross section, and $C_{\Lambda\Lambda}$ by fitting the chiral EFT phase shift.

J. Haidenbauer, Ulf-G. Meißner, and S. Petschauer, Nucl. Phys. A 954, 273 (2016).

$N\Lambda$

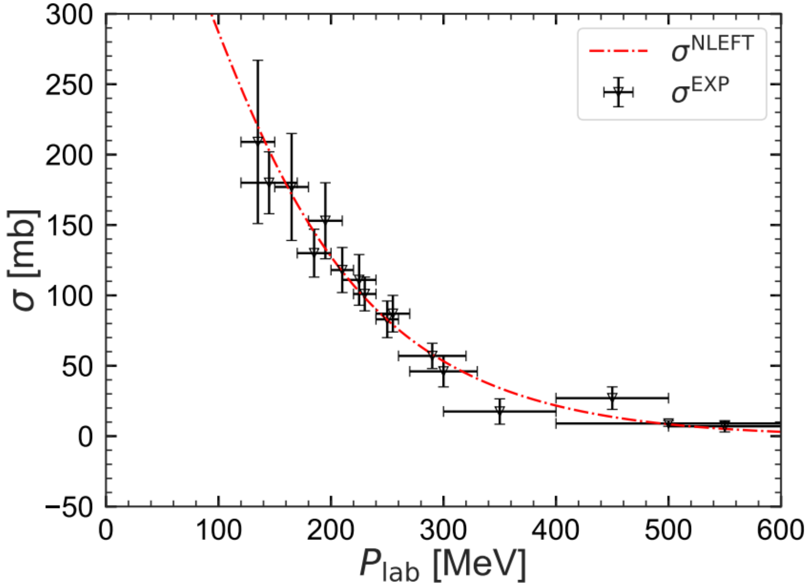

$\Lambda\Lambda$

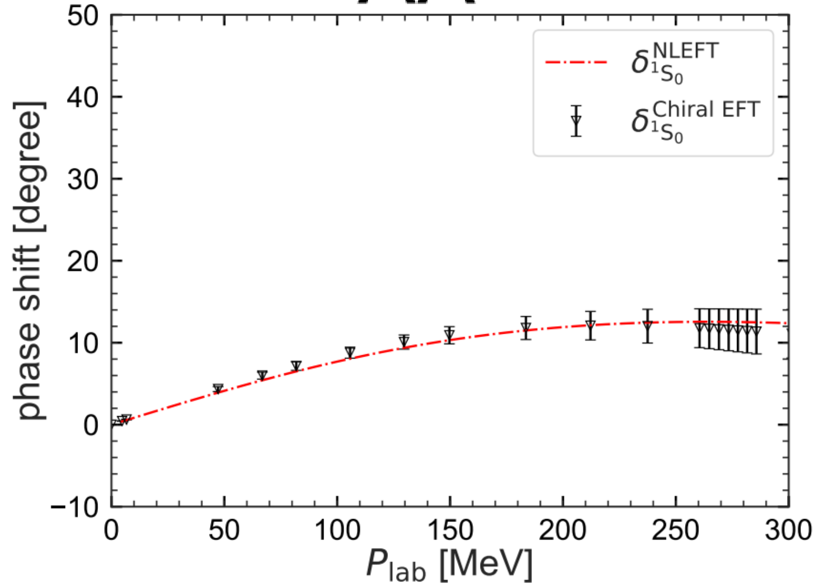

- The LECs of the $NN\Lambda$ and $N\Lambda\Lambda$ three-baryon forces are constrained by the separation energy of light hypernuclei $^{5}_{\Lambda}\mathrm{He}$, $^{8}_{\Lambda}\mathrm{Be}$, $^{9}_{\Lambda}\mathrm{Be}$, $^{6}_{\Lambda\Lambda}\mathrm{He}$, and $^{10}_{\Lambda\Lambda}\mathrm{Be}$

$$B_\Lambda(^A_\Lambda Z) = E(^{A-1}Z) - E(^A_\Lambda Z),$$
$$B_{\Lambda\Lambda}(^A_{\Lambda\Lambda} Z) = E(^{A-2}Z) - E(^A_{\Lambda\Lambda} Z).$$

Hypernuclei

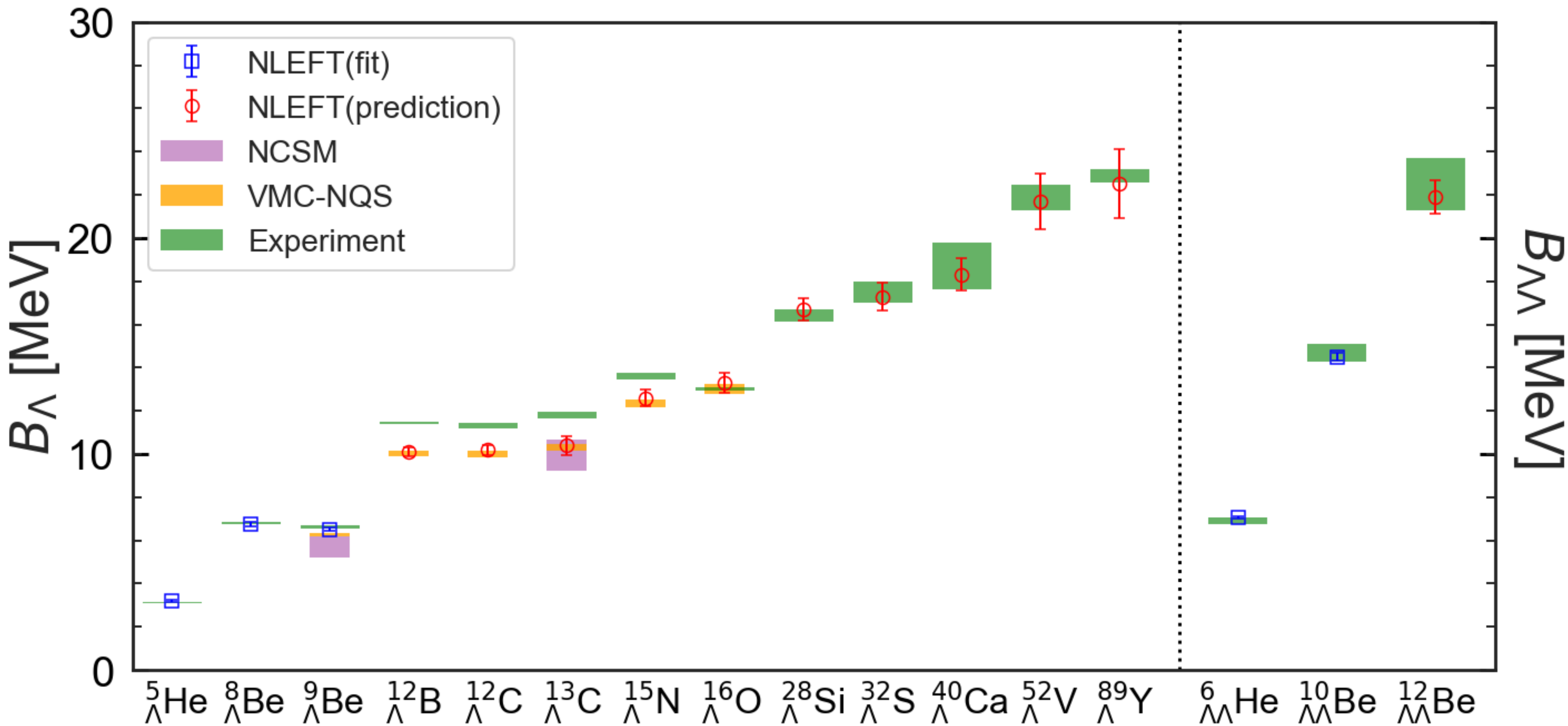

☼ *Hui Tong, Serdar Elhatisari, Ulf-G. Meißner, and Zhengxue Ren, arXiv.2509.26148(2025)*

① NCSM : N3LO chiral EFT interaction for nucleons and the LO NΛ force, without explicit NNΛ three-body force. ☼ *M. Knöll and R. Roth, PLB 846, 138258 (2023)*

② VMC-NQS : variational Monte Carlo based on neural network quantum states + LO pionless EFT. ☼ *A. D. Donna, et al., arXiv: 2507, 16994 (2025)*

③ NLEFT : our results are close to experimental data.

Neutron star EoS

- The energy density can be obtained as

$$\varepsilon_{\mathrm{HNM}} = \rho \left[\frac{E_{\mathrm{HNM}}(x_n, x_p, x_\Lambda)}{N_{\mathrm{tot}}} + x_n m_n + x_p m_p + x_\Lambda m_\Lambda + e_e + e_\mu \right],$$

the chemical potentials are evaluated via

$$\mu_n(\rho, x_p, x_\Lambda) = \frac{\partial \varepsilon_{\mathrm{HNM}}}{\partial \rho_n}, \quad \mu_p(\rho, x_p, x_\Lambda) = \frac{\partial \varepsilon_{\mathrm{HNM}}}{\partial \rho_p}, \quad \mu_\Lambda(\rho, x_p, x_\Lambda) = \frac{\partial \varepsilon_{\mathrm{HNM}}}{\partial \rho_\Lambda},$$

the particle fractions, $x_i(\rho)$, with $i = n, p, \Lambda$, are determined by imposing the chemical-equilibrium condition

$$\mu_n = \mu_\Lambda, \qquad \mu_n - \mu_p = \mu_e, \qquad \mu_e = \mu_\mu,$$

together with charge neutrality. The pressure is defined as

$$P(\rho) = \rho^2 \frac{d}{d\rho} \frac{\varepsilon_{\mathrm{HNM}}}{\rho}.$$

Energy for hypernuclear matter

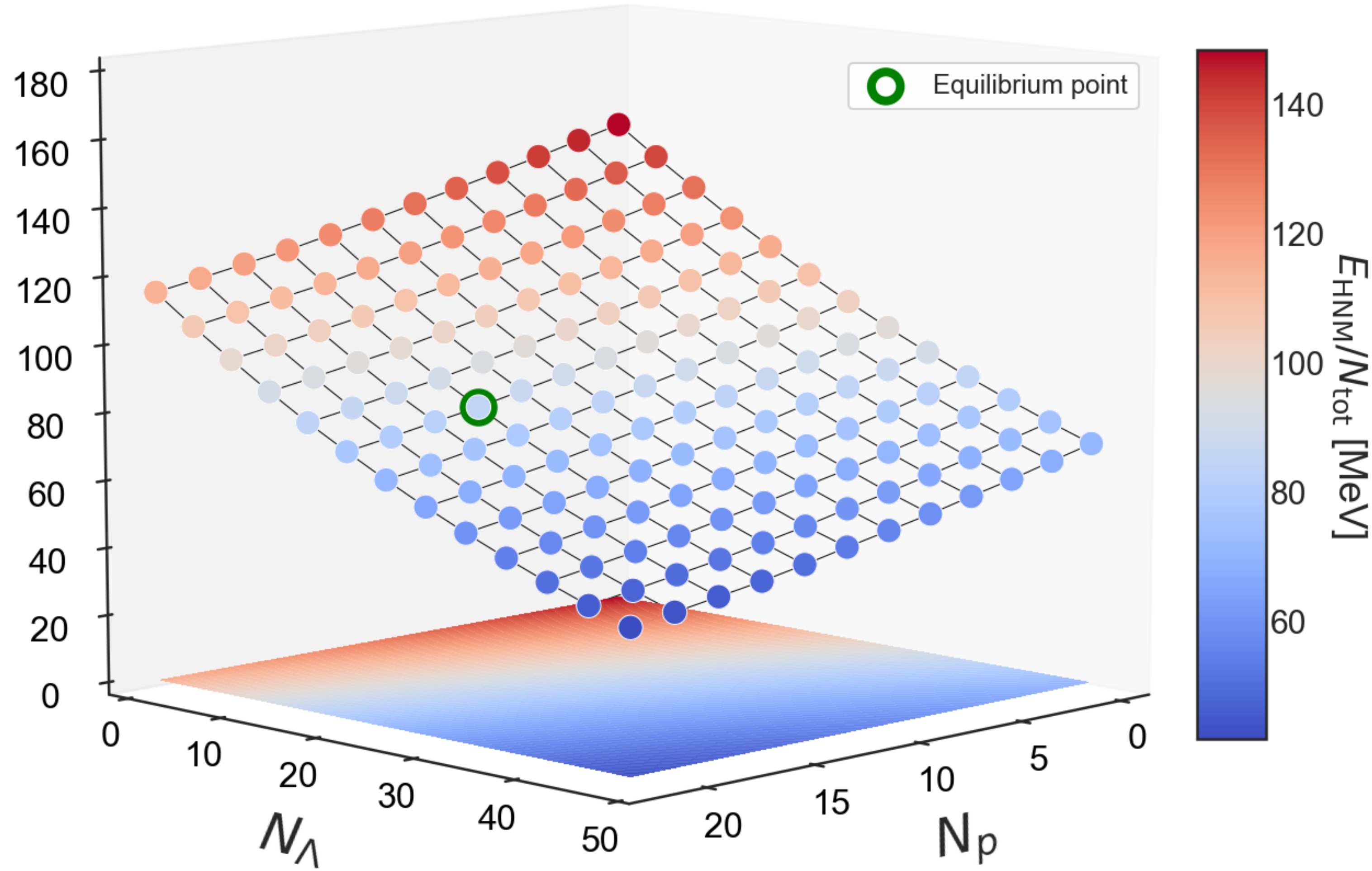

① The first *ab initio* Monte Carlo simulations for an arbitrary number of neutrons, protons, and Λ hyperons.

② The energy per baryon decreases as either N_p or N_Λ increases, the green circle indicates the equilibrium point of β-stable matter.

The particle fractions

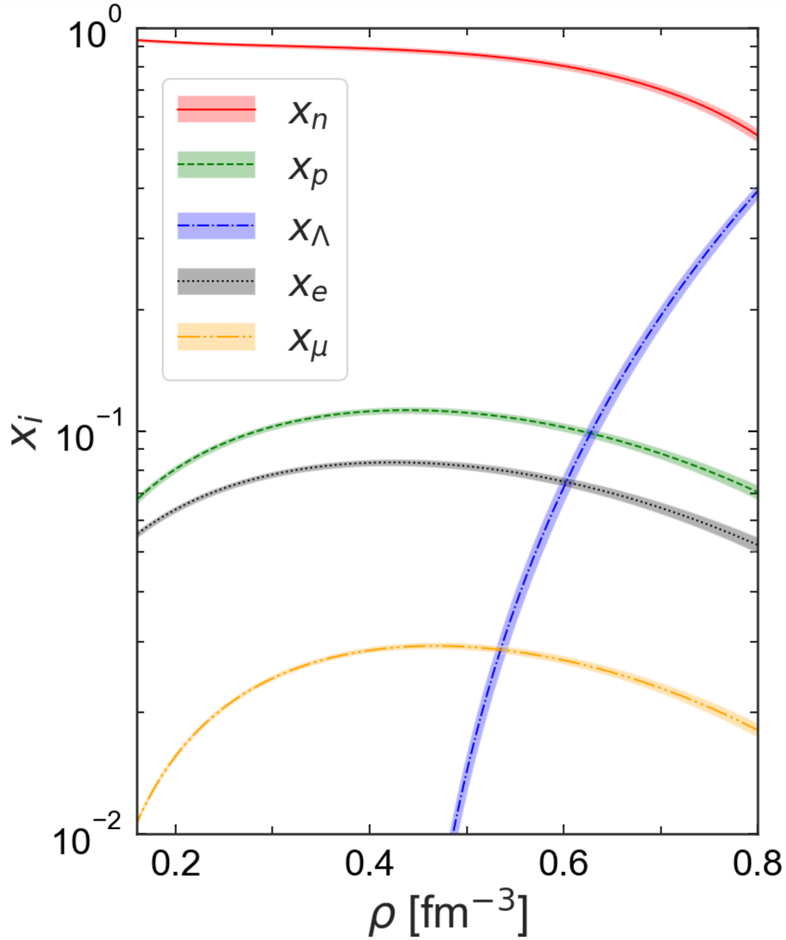

① With increasing density, the proton fraction rises to values above 10% before gradually decreasing at higher densities .

② The behavior is in full qualitative agreement with earlier microscopic BHF theory employing the $N\Lambda$ interaction from the Nijmegen Soft-Core 97 (NSC97) potential.

☼ *D. Logoteta, et al., Eur. Phys. J. A 55, 207 (2019)*

EoS for hypernuclear matter

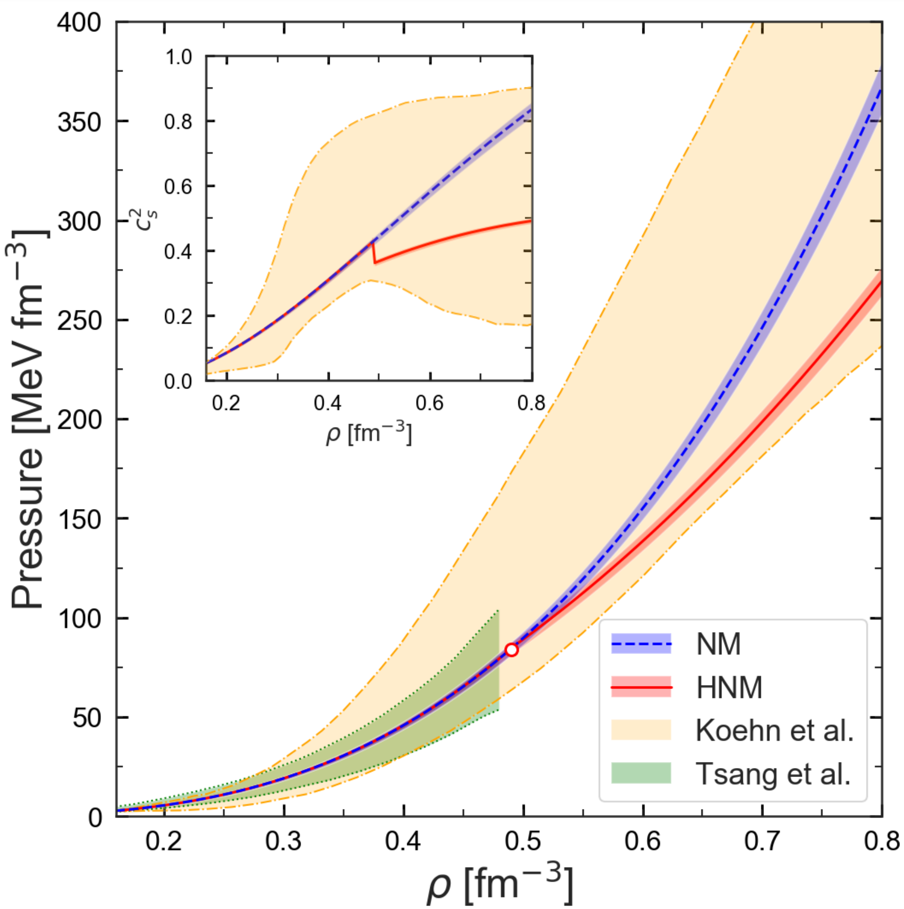

① The threshold density : $\rho_\Lambda^{\mathrm{th}} = 0.490(2)(5)\ \mathrm{fm}^{-3}$.

② The orange regions are constrained by chiral EFT, pQCD, and astrophysical observations.

☼ *Hauke Koehn, et al., PRX 15, 021014 (2025)*

③ The green regions are constrained by astrophysical observations together with nuclear experimental data.

☼ *Tsang, et al., Nature Astron. 8, 328 (2024)*

Trace anomaly

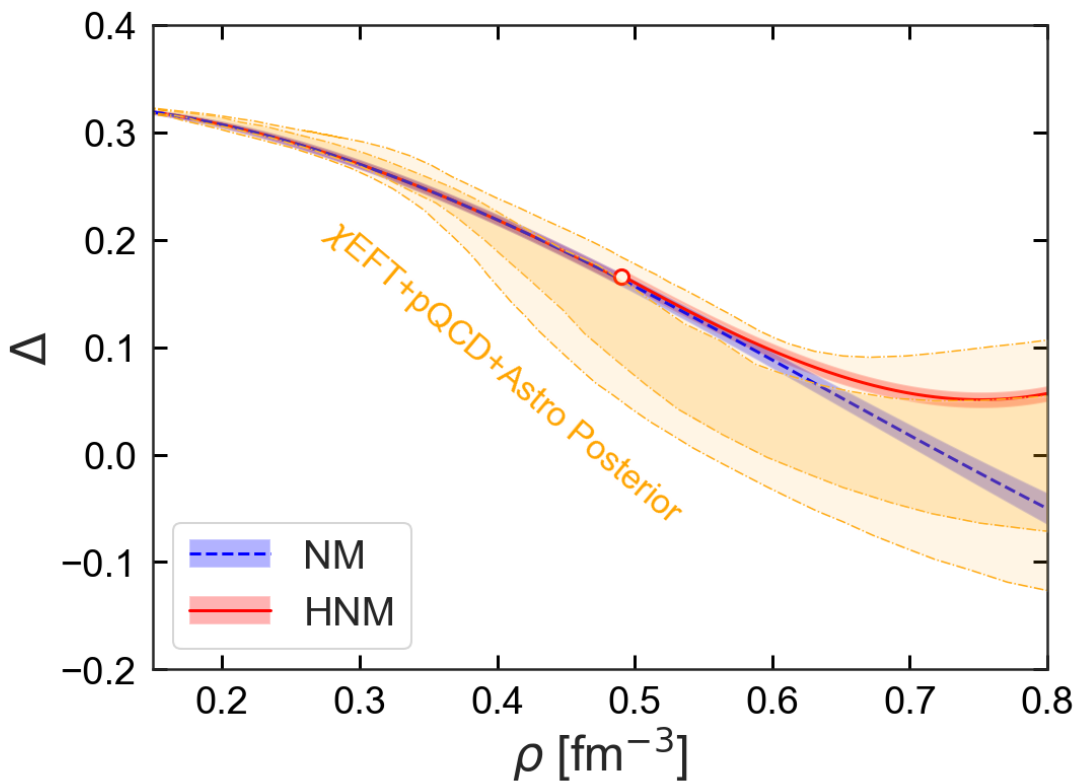

① The normalized trace anomaly $\Delta = 1/3 - P/\varepsilon$ serves as a key measure of conformality in dense matter.

② The inclusion of hyperons shifts Δ upward relative to NM, reflecting the softening of the EoS due to additional degrees of freedom.

③ Our results remain within the credible intervals from Bayesian analyses.

☼ *E. Annala, et al., Nature Communications 14, 8451 (2023)*

Neutron star properties

- Tolman-Oppenheimer-Volkoff (TOV) equations

☼ *R. C. Tolman, Phys. Rev. 55, 364 (1939)* ☼ *J. R. Oppenheimer and G. M. Volkoff, Phys. Rev. 55, 374 (1939)*

$$\boxed{\begin{aligned}\frac{dP(r)}{dr} &= -\frac{[P(r)+\varepsilon(r)][M(r)+4\pi r^3 P(r)]}{r[r-2M(r)]},\\ \frac{dM(r)}{dr} &= 4\pi r^2 \varepsilon(r),\end{aligned}}$$

where $P(r)$ is the pressure, and $M(r)$ is the total star mass.

- Neutron star tidal deformability Λ

☼ *E. E. Flanagan and T. Hinderer, PRD 77, 021502 (2008)* ☼ *T. Hinderer, ApJ 677, 1216 (2008)*

$$\boxed{\Lambda = \frac{2}{3} k_2 \left(\frac{R}{M}\right)^5,}$$

which represents the mass quadrupole moment response of a neutron star to the strong gravitational field induced by its companion, k_2 is the second Love number.

Neutron star mass and radius

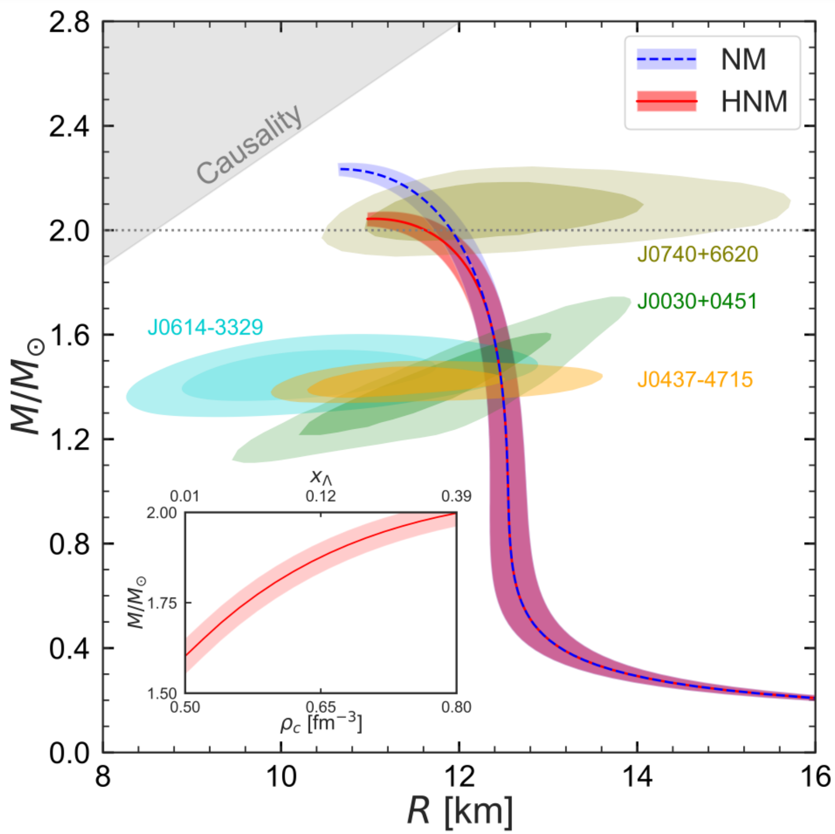

① The maximum mass for HNM: M_{max}=2.04(1)(2)$M_\odot$.

② The inclusion of hyperons significantly lowers the maximum mass compared with the purely nucleonic case, the predicted curves remain fully compatible with the neutron star observations.

③ The Λ fraction rises steadily with increasing mass, reaching as high as 39% in the core of a $2M_\odot$ star.

Neutron star tidal deformability

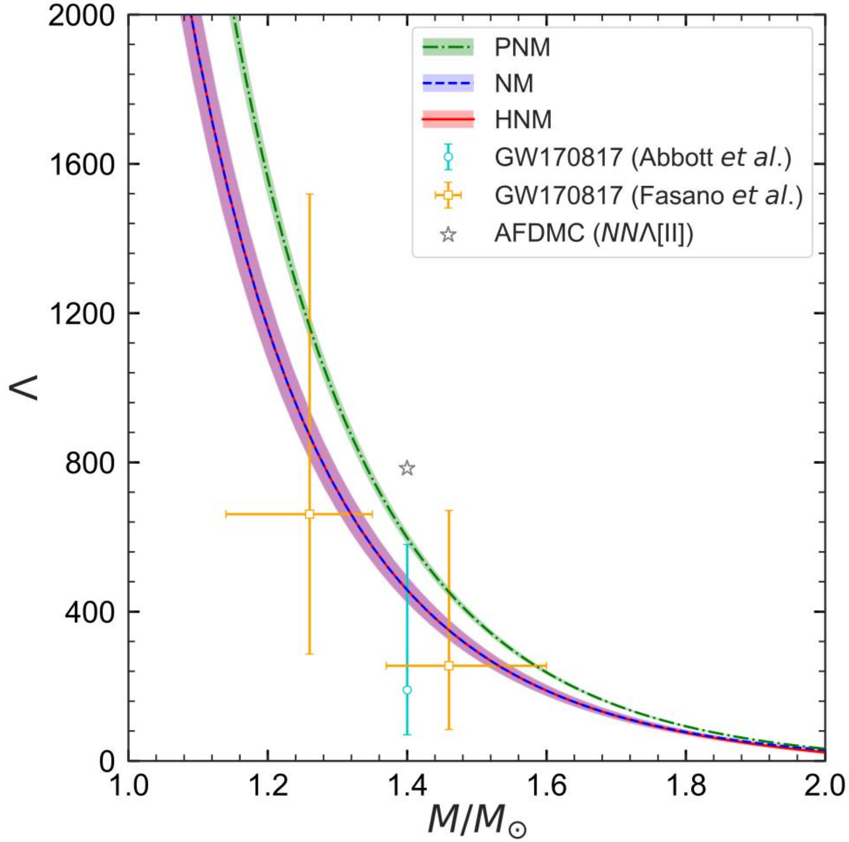

☼ *B. P. Abbott, et al., PRL 121, 161101 (2018)*

☼ *M. Fasano, et al., PRL 123, 141101 (2019)*

① The PNM EoS is overly stiff and yields $\Lambda_{1.4M_\odot}$ values above the ranges inferred from GW170817.

② Once protons are consistently included in β-equilibrium, the EoS softens and the predicted tidal deformabilities fall in line with the observational constraints.

③ The EoS is overly stiff and clearly incompatible with astrophysical observations from AFDMC calculations using their second parametrization of the $NN\Lambda$ force.

Contents

Summary and Outlook

① By combining NLEFT with a novel AFQMC algorithm, we have carried out the first sign-problem free *ab initio* MC simulations containing arbitrary number of neutrons, protons and Λ hyperons, consistently incorporating all relevant two- and three-body forces.

② We have presented the first *ab initio* calculations that achieve a unified description of single- and double-Λ hypernuclei from light to medium-mass systems, the EoS of β-stable hypernuclear matter, and neutron star properties.

③ Our results show that $2M_\odot$ neutron stars can accommodate substantial hyperon fractions—up to nearly 40% in the stellar core—in contrast to earlier AFDMC studies that ruled out hyperons to satisfy the mass constraint.

In the next step,

① We will use the recently developed hi-fidelity chiral interactions at N3LO and include other hyperons in our simulations.

☼ *S. Elhatisari , et al., Nature 630, 59 (2024)*

Thanks for your attention !

Appendix

Universal relations I-Love-Q

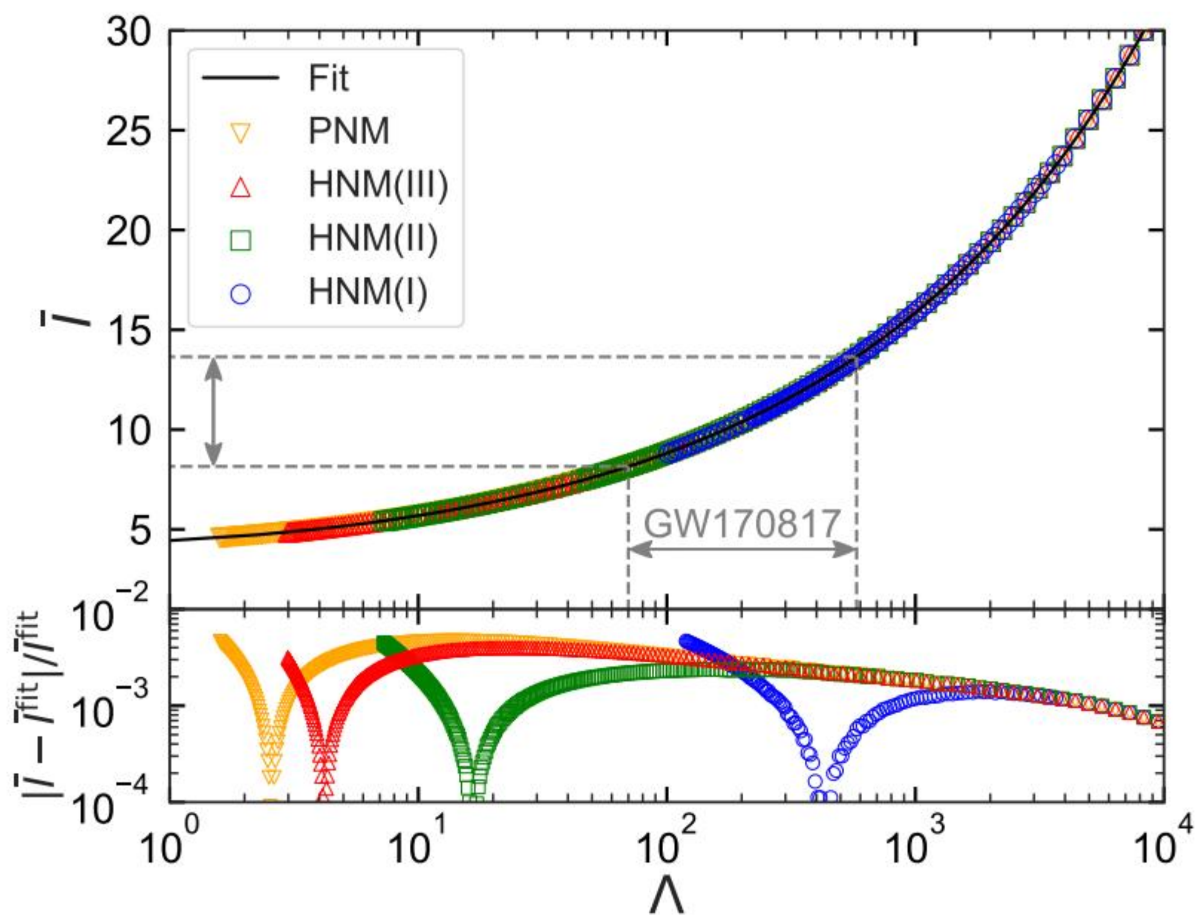

① $\bar{I}$ is the dimensionless quantities for the moment of inertia, 8.2<$\bar{I}$<13.7

② Fitting function

☼ *K. Yagi and N. Yunes, Science 341, 365 (2013)*

$$\ln y_i = a_i + b_i \ln x_i + c_i (\ln x_i)^2 + d_i (\ln x_i)^3 + e_i (\ln x_i)^4$$

Rotating Neutron Star

- Rotation causes an NS to deform into an oblate spheroid, resulting in a larger equatorial radius and an increased gravitational mass compared to a non-rotating NS, which is related to an increase of the centrifugal force.

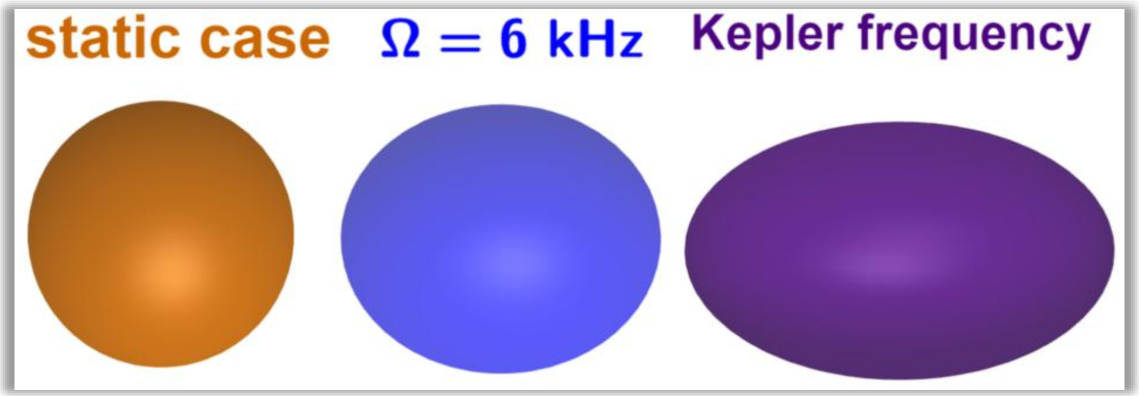

C. Gartlein, arXiv:2412.07758 (2024)

The rapidly rotating neutron star can be described by the energy-momentum tensor:

$$\boxed{T^{\mu\nu} = (\varepsilon + P)u^\mu u^\nu - g^{\mu\nu} P,}$$

where u^μ is the fluid's four-velocity.

Rotating Neutron Star Properties

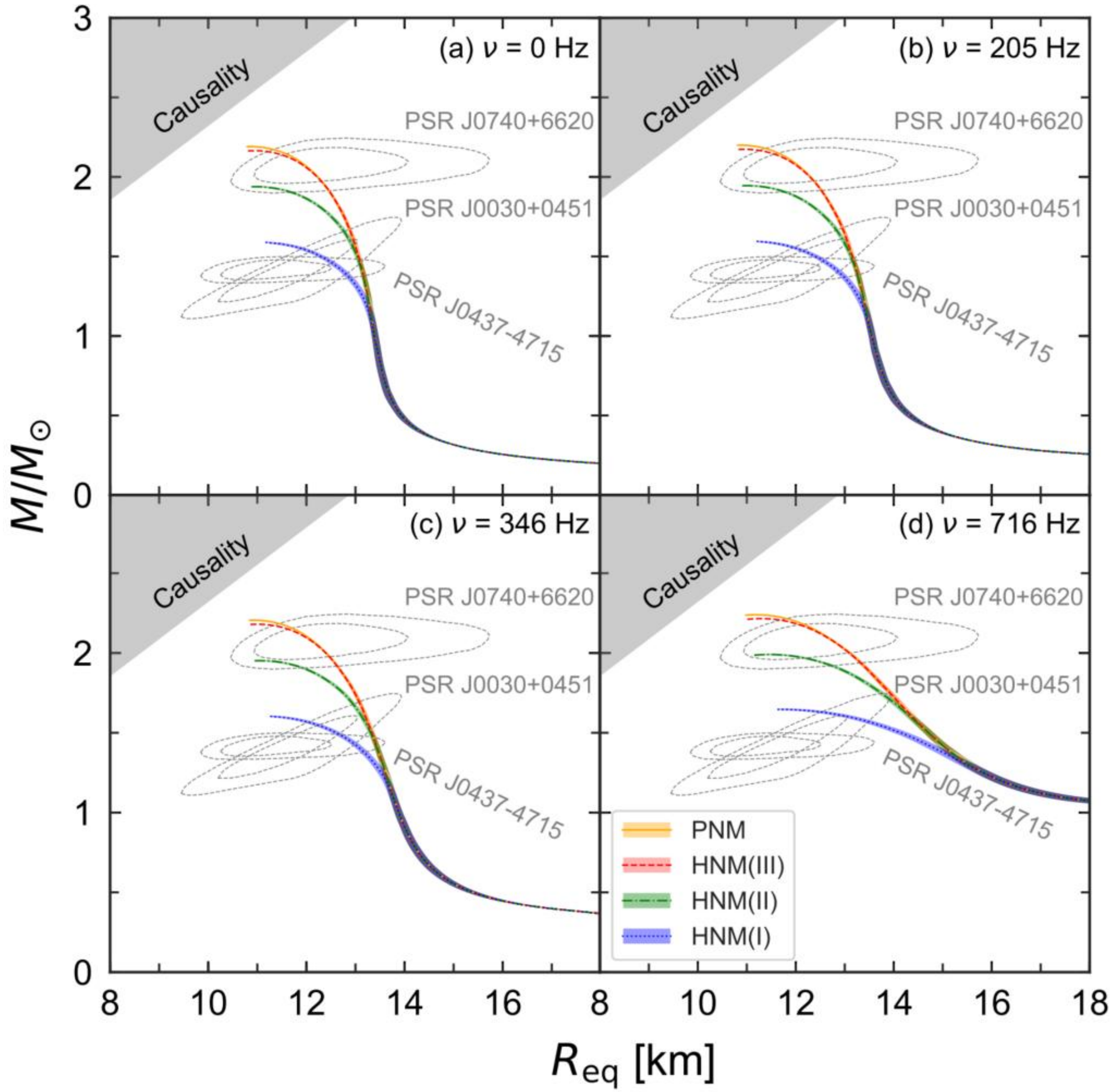

① Four constant spin frequencies ν = 0, 205, 346, 716 Hz are shown

② The impact of rotational dynamics on the maximum mass is small

Hyper β-stable nuclear matter

- The equilibrium conditions and the charge neutrality condition,

$$\mu_n - \mu_p = \mu_e, \quad \mu_e = \mu_\mu, \quad \mu_n = \mu_\Lambda, \quad \rho_p = \rho_e + \rho_\mu.$$

Incorporating protons significantly increases the computational. For example, at $\rho = 0.5\ \mathrm{fm}^{-3}$ (the total number of baryons are 142),

Hyper-neutron matter	Hyper β-stable nuclear matter
108 jobs	1620 jobs

Symmetry energy and EoS

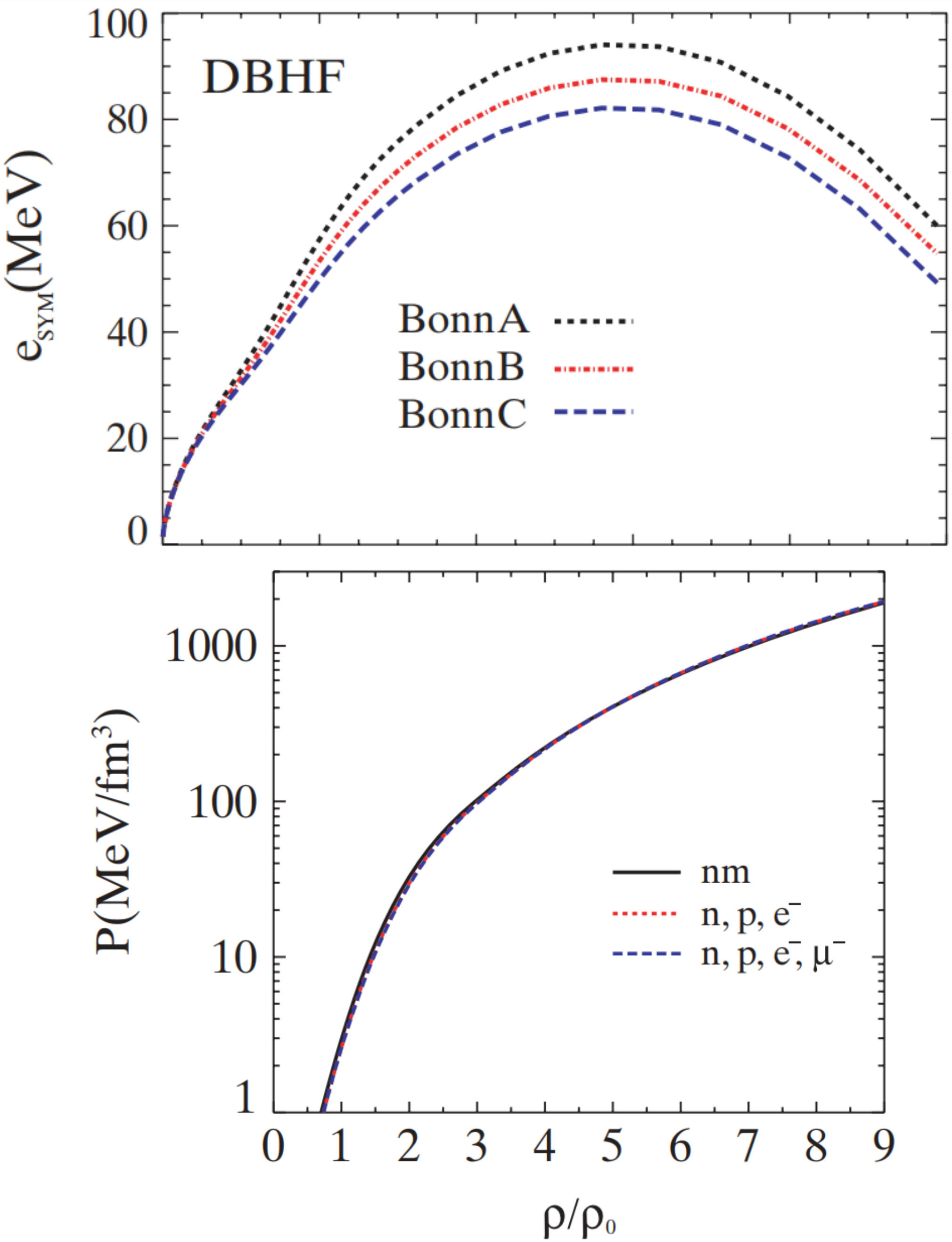

☼ *Physical Review C 74, 025808 (2006)*

I-Love-Q (II)

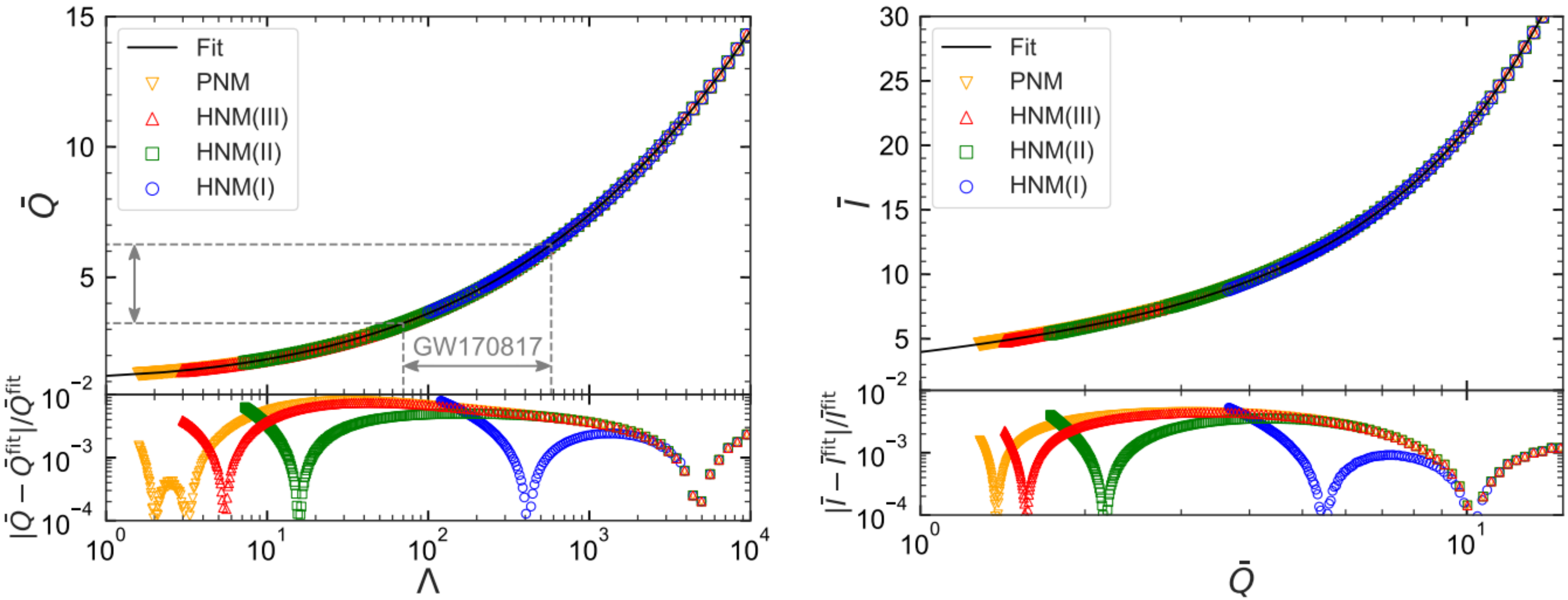

TABLE III. Numerical coefficients for the fit formula of the I-Love, I-Q, and Q-Love relations.

y_i	x_i	a_i	b_i	c_i	d_i	e_i
$\bar{I}$	Λ	1.49093×10^{0}	5.93880×10^{-2}	2.24914×10^{-2}	-6.93727×10^{-4}	7.78146×10^{-6}
$\bar{Q}$	Λ	1.97175×10^{-1}	9.19620×10^{-2}	4.93555×10^{-2}	-4.56214×10^{-3}	1.39647×10^{-4}
$\bar{I}$	$\bar{Q}$	1.40269×10^{0}	5.25610×10^{-1}	4.07856×10^{-2}	1.85656×10^{-2}	1.00574×10^{-4}

☼ *J. J. Li, A. Sedrakian, and F. Weber, Phys. Rev. C 108, 025810 (2023).*

EOS from different information channels

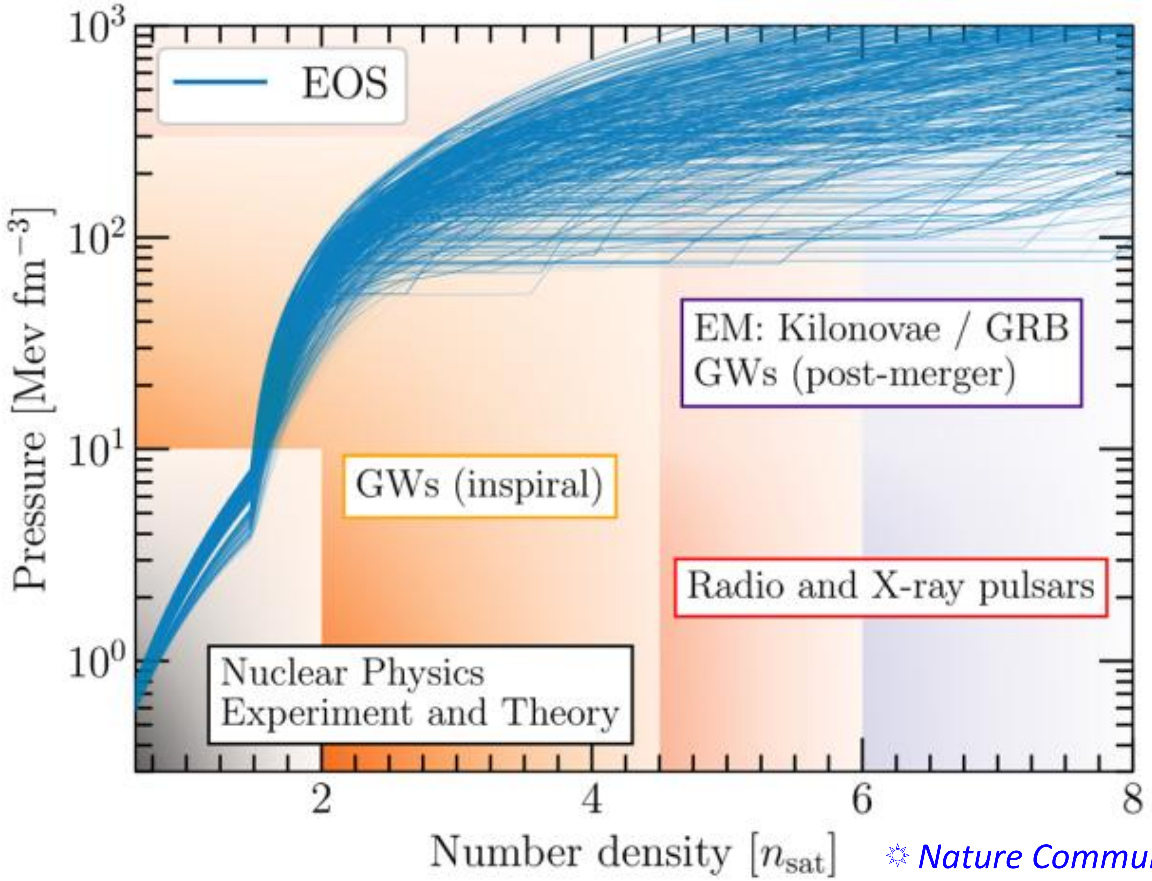

☼ *Nature Communications 14, 8352 (2023)*

Fig. 1 | Overview of constraints on the EOS from different information channels. We show a set of possible EOSs (blue lines) that are constrained up to $1.5n_{sat}$ by Quantum Monte Carlo calculations using chiral EFT interactions[80] and extended to higher densities using a speed of sound model[149]. Different regions of the EOS can then be constrained by using different astrophysical messengers, indicated by rectangulars: GWs from inspirals of NS mergers, data from radio and X-ray pulsars, and EM signals associated with NS mergers. Note that the boundaries are not strict but depend on the EOS and properties of the studied system.

Finite volume

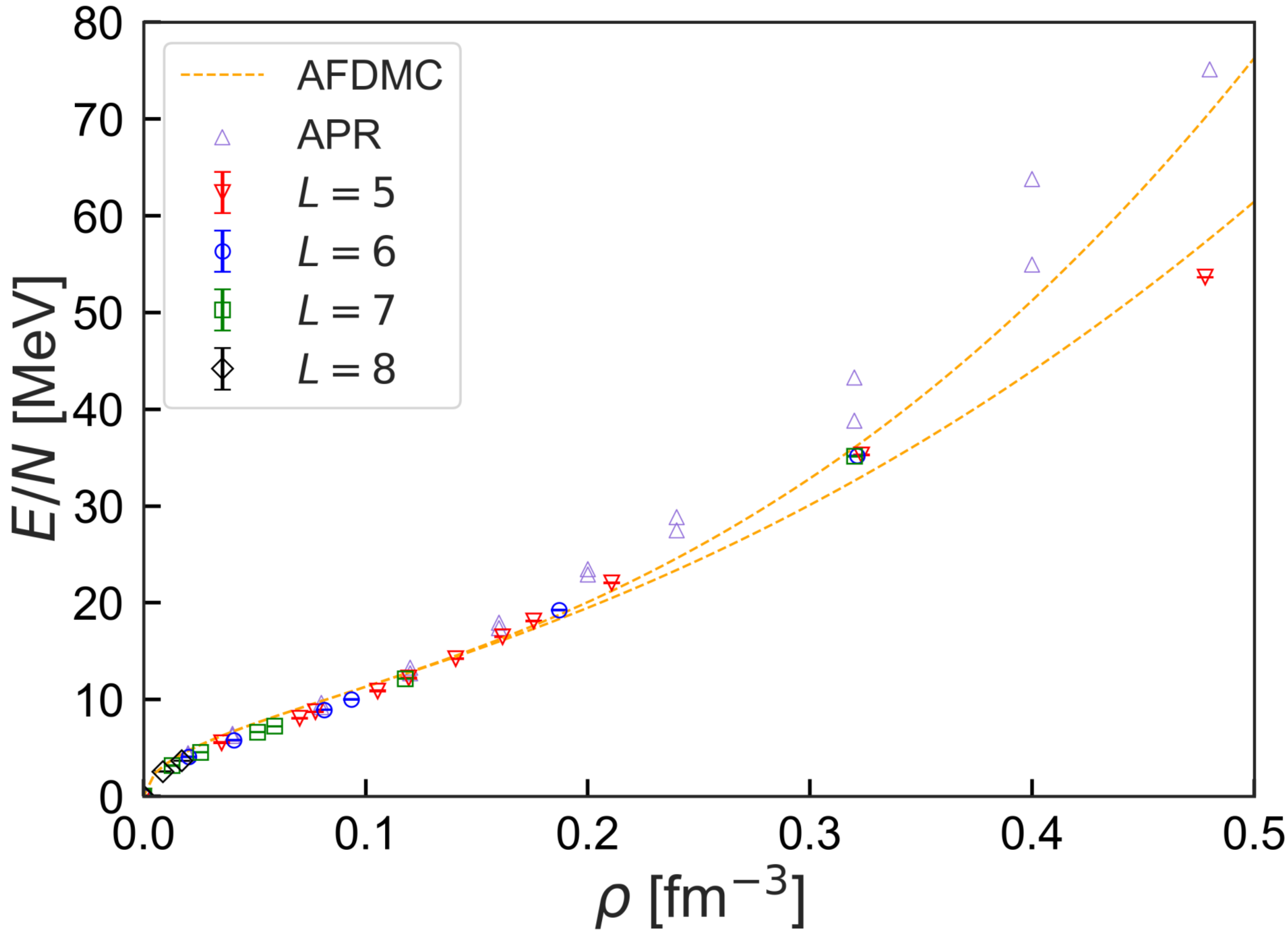

Gerstung et al's work

Next, we compare our work with the one of Gerstung et al. [17]. For the ΛN interaction, they consider two next-to-leading order chiral EFT representations, called NLO13 [95] and NLO19 [96]. For the three-body forces, they use the leading ΛNN representation based on chiral EFT (contact terms, one-pion and two-pion exchanges) with the inclusion of the $\Lambda NN \leftrightarrow \Sigma NN$ transition [97] in an effective density-dependent two-body approximation [98]. The pertinent LECs are given in terms of decuplet resonance saturation and leave one with two B^*BBB couplings, where B denotes the baryon octet and B^* the decuplet. If one only considers the ΛNN force as we do, these two LECs appear in the combination $H' = H_1 + H_2$. No $\Lambda\Lambda N$ force was considered in [17]. The two LECs H_1, H_2 where constrained in[17] so that the Λ single-particle potential in infinite matter is $U_\Lambda(\rho \simeq \rho_0) = -30$ MeV [5]. Due to numerical instabilities in calculation of the Brueckner G-matrix, the computation can only be done up to densities $\rho \simeq 3.5\rho_0$. The authors of Ref. [17] then use a quadratic polynomial to extrapolate to higher densities. They calculate the chemical potential for the neutrons and Λs from the Gibbs-Duhem relation using a microscopic EoS computed from a chiral nucleon-meson field theory in combination with functional renormalization group methods. The parameter combinations $(H_1,\ H_2)$ were chosen so that the Λ single-particle potential becomes maximally repulsive at higher densities. The resulting chemical potentials are displayed in Fig. 10 for the NLO19 ΛN forces. These agree well with the HNM(III) chemical potentials up to $\rho \simeq 2.5\rho_0$ but show, different to what we find, no crossing. Note that the forces discussed in [17] have not been applied to finite nuclei.

2B and 3B interaction in AFDMC

For the hyperon sector, we adopted the phenomenological hyperon-nucleon potential that was first introduced by Bodmer, Usmani, and Carlson in a similar fashion to the Argonne and Urbana interactions [44]. It has been employed in several calculations of light hypernuclei [45–51] and, more recently, to study the structure of light and medium mass Λ hypernuclei [34,35]. The two-body ΛN interaction, $v_{\lambda i}$, includes central and spin-spin components and it has been fitted on the available hyperon-nucleon scattering data. A charge symmetry breaking term was introduced in order to describe the energy splitting in the mirror Λ hypernuclei for $A = 4$ [34,47]. The three-body ΛNN force, $v_{\lambda ij}$, includes contributions coming from P- and S-wave 2π exchange plus a phenomenological repulsive term. In this work we have considered two different parametrizations of the ΛNN force.

The authors of Ref. [49] reported a parametrization, hereafter referred to as parametrization (I), that simultaneously reproduces the hyperon separation energy of ${}^{5}_{\Lambda}$He and ${}^{17}_{\Lambda}$O obtained using variational Monte Carlo techniques. In Ref. [34], a diffusion Monte Carlo study of a wide range of Λ hypernuclei up to $A = 91$ has been performed. Within that framework, additional repulsion has been included in order to satisfactorily reproduce the experimental hyperon separation energies. We refer to this model of ΛNN interaction as parametrization (II).

No $\Lambda\Lambda$ potential has been included in the calculation. Its determination is limited by the fact that $\Lambda\Lambda$ scattering data are not available and experimental information about double Λ hypernuclei is scarce. The most advanced theoretical works discussing $\Lambda\Lambda$ force [52,53], show that it is indeed rather weak. Hence, its effect is believed to be negligible for the purpose of this work. Self-bound multi-strange systems have been investigated within the relativistic mean field framework [54–56]. However, hyperons other than Λ have not been taken into account in the present study due to the lack of potential models suitable for quantum Monte Carlo calculations.

Parameterization in AFDMC

$\rho_\Lambda = x\rho$ are the neutron and hyperon densities, respectively. The energy per particle can be written as

$$E_{\rm HNM}(\rho, x) = [E_{\rm PNM}((1-x)\rho) + m_n](1-x) + [E_{\rm P\Lambda M}(x\rho) + m_\Lambda]x + f(\rho, x). \qquad (2)$$

We parametrized the energy of pure lambda matter $E_{\rm P\Lambda M}$ with the Fermi gas energy of noninteracting Λ particles. Such a formulation is suggested by the fact that in the Hamiltonian of Eq. (1) there is no $\Lambda\Lambda$ potential. The reason for parametrizing the energy per particle of hyperneutron matter as in Eq. (2) lies in the fact that, within AFDMC calculations, $E_{\rm HNM}(\rho, x)$ can be easily evaluated only for a discrete set of x values. They correspond to a different number of neutrons ($N_n = 66, 54, 38$) and hyperons ($N_\Lambda = 1, 2, 14$) in the simulation box giving momentum closed shells. Hence, the function $f(\rho, x)$ provides an analytical parametrization for the difference between Monte Carlo energies of hyperneutron matter and pure neutron matter in the (ρ, x) domain that we have considered. Corrections for the finite-size effects due to the

EoS(S=-2)

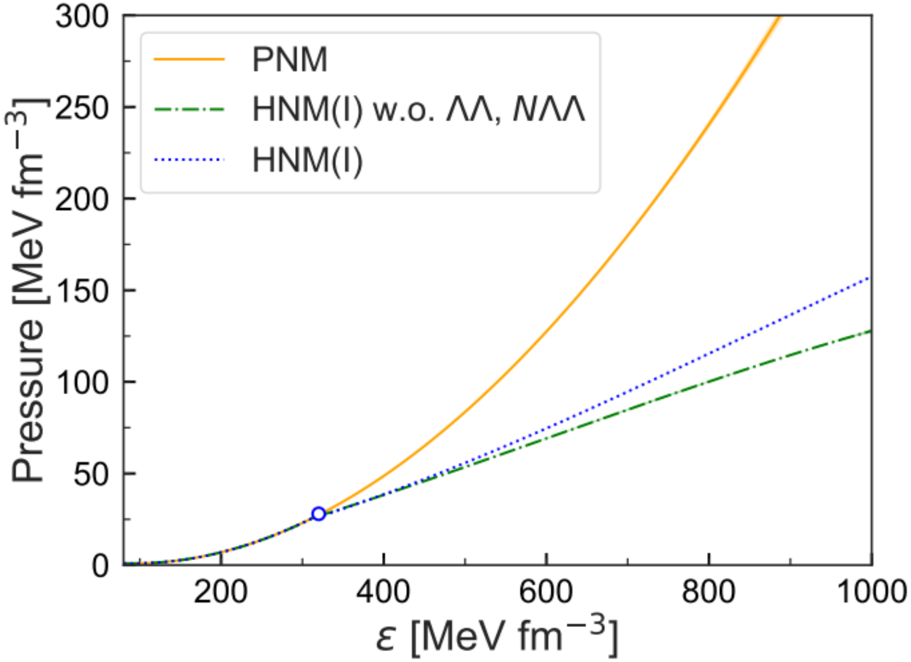

PNM
HNM(I) w.o. ΛΛ, NΛΛ
HNM(I)
Pressure [MeV fm^{-3}]
ε [MeV fm^{-3}]
0
50
100
150
200
250
300
200
400
600
800
1000

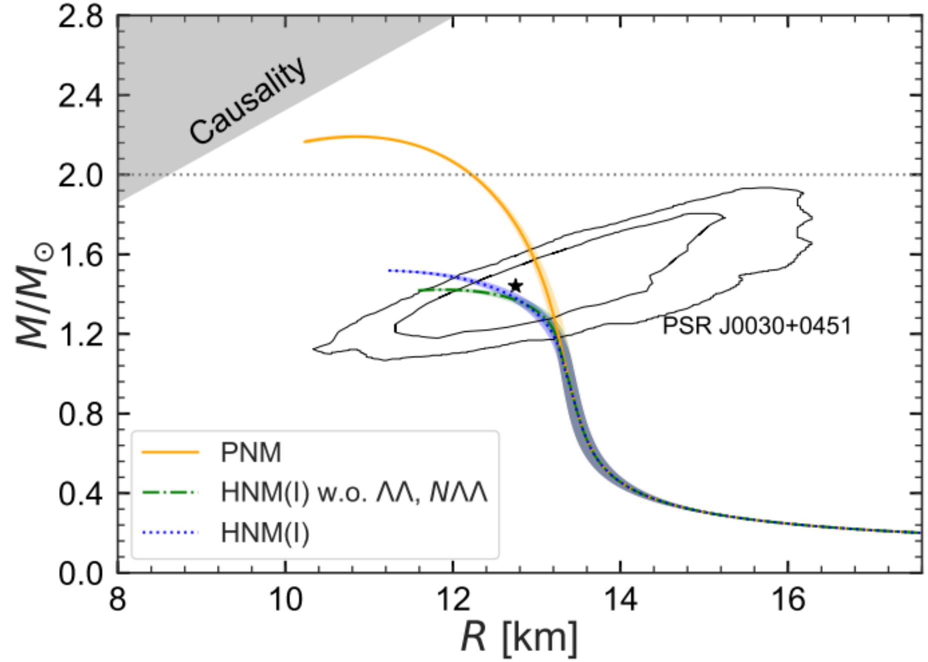

Causality
PSR J0030+0451
PNM
HNM(I) w.o. ΛΛ, NΛΛ
HNM(I)
$M/M_\odot$
R [km]
0.0
0.4
0.8
1.2
1.6
2.0
2.4
2.8
8
10
12
14
16